Investigation of Oxidative Stress and Mitochondrial Damage on Rat Derived Neural Stem Cells in 3D Organoid Models

Onur Özcan
Department of Stem Cell, Institute of Health Sciences, Kocaeli University
Yusufhan Yazır
yusufhanyazir@yahoo.com
Center for Stem Cell and Gene Therapies Research and Practice, Kocaeli University
Gökhan Duruksu
Center for Stem Cell and Gene Therapies Research and Practice, Kocaeli University
Ahmet Öztürk
Department of Stem Cell, Institute of Health Sciences, Kocaeli University
Kamil Can Kılıç
Department of Stem Cell, Institute of Health Sciences, Kocaeli University

Research Article

Keywords: Neural Stem Cells, Organoid, Hydrogen Peroxide, Mitochondria, Oxidative Stress

Posted Date: September 3rd, 2024

DOI: https://doi.org/10.21203/rs.3.rs-4873168/v1

Additional Declarations: No competing interests reported.

Investigation of Oxidative Stress and Mitochondrial Damage on Rat Derived Neural Stem Cells in 3D Organoid Models

Abstract

Our goal was to investigate mitochondrial damage in a three-dimensional (3D) neural stem cell (NSC) organoid model using oxidative stress-induced NSCs as primary research method. To create an in vitro organoid model, we utilized NSCs that were exposed to oxidative stress by treating them with hydrogen peroxide (H_2O_2) at a concentration of 75 μM, leading to mitochondrial damage. Markers for oxidative stress, differentiation, and neurodegenerative diseases were analyzed to characterize organoid models by assessing gene expression and protein levels via histology, immunofluorescence staining, spectrophotometry, and Real-Time PCR. To determine extent of mitochondrial damage in organoid models, we compared mitochondrial membrane potential and total mitochondrial ratio. We independently evaluated mitochondrial damage in both spontaneously self-organized organoid model and oxidative stress organoid models. The 3D NSC organoid model was established through histological and immunofluorescent analyses, which revealed a well-organized cellular structure. Due to intentionally induced oxidative stress, cell distribution varied. We found that H_2O_2 reduced cell viability and stimulated proliferation at specific concentrations. The cells in oxidative stress model showed strong expression of neural markers MAP2 and TUBB3 compared to controls, as well as positive expression of Alzheimer's marker TAU on 28^{th} day. The model also displayed mitochondrial membrane changes and increased mitophagy during culture process. Overall, we successfully developed an organoid model using multipotent NSCs, which demonstrated H_2O_2's crucial role in directing cell differentiation and behavior. The model exhibited expected matrix rearrangement, resembling typical organoids, suggesting its potential as an Alzheimer's model and utility in related research studies.

Keywords: Neural Stem Cells, Organoid, Hydrogen Peroxide, Mitochondria, Oxidative Stress

Introduction

Stem cells exhibit capacity to proliferate indefinitely and differentiate into a variety of cell types, from initial stages of development until end of life. They are specialized cells that possess unique characteristics that distinguish them from other cell groups, including ability to self-renew and differentiate into different cell types, as well as their capacity to form clones (Sangkum, 2016). These cells are the primary components of all tissues and organs in body and possess the ability to divide and self-renew continuously, as well as to differentiate into various organs and tissues. Recent advances in neural stem cell research have established widely accepted notion that adult neural stem cells (aNSCs) are specifically located in subventricular zone (SVZ) of lateral ventricular wall and subgranular zone (SGZ) of hippocampal dentate gyrus. (Gage 2000; Zhao et al. 2008). In adult brain's SVZ, a population of quiescent aNSCs is believed to reside beneath ependymal layer and make contact with the ventricle through their apical surface. These cells have been characterized as expressing LeX, CD133, GFAP, and Nestin, and are negative for differentiated cell markers such as CD24, O4, NeuN, and S100β. A similar subset of GFAP+, S100β-, Sox2+, Nestin+ radial cells, known as silent NSCs, are present in SGZ region of dentate gyrus. The characteristics of aNSCs have been well-defined and these cells have capable of differentiating into all subtypes of oligodendrocytes and into nervous system cell types and repopulate damaged areas of nervous system.

Neurodegenerative diseases cause a great threat to human health (Gitler et al. 2017). These disorders are generally correlated with aging and oxidative stress due to becoming increasingly common in number of elderly population in recent years (Jaul, 2017). Although there are some theories on aging at cellular level, it is not known about how microscopic failures cause macroscopic damages of tissues, organs, and ultimately the organism. 3D cell culture techniques are becoming increasingly common (Langharns, 2018; Ekert et al. 2014; Finnberg et al. 2017). Recent advances in stem cell and mammalian developments in biology have also significantly increased use of these techniques in literature (Zakrzewski et al. 2019; Chen et al. 2014). 3D cultivation of both pluripotent and differentiated cells reveal critical natural features missing in standard two-dimensional (2D) cultivation. Unlike 2D standard culture technique 3D culture conditions can create various cellular phenotypes depending on to niche microenvironment, polarity, and ECM interplay. Cell-derived tissue and organ-like structures that contain one or more cell types are called organoids. Totipotent cells such as embryonic stem cells, pluripotent IPS cells or multipotent featured stem cells can be used when creating organoid cultures. Neural stem/precursor cells are involved in brain development and self-renewal processes in adult mammalian brain. In addition, these cells can differentiate into neurons, astrocytes, and oligodendrocytes in vitro (McKay, 1997).

Neurodegenerative disorders like Alzheimer's, Parkinson's, and amyotrophic lateral sclerosis are linked to oxidative stress and mitochondrial damage. This damage arises from an imbalance between free radicals and the body's antioxidant defenses, either due to increased free radicals or decreased antioxidant enzymes. Enzymes such as iron-sulfur and flavoproteins can reduce oxygen to highly toxic superoxide radicals, causing cell damage. Oxidative stress significantly affects biological processes, especially apoptosis, and is a major factor in many diseases. It leads to excessive reactive oxygen species, resulting in mitochondrial DNA mutations, respiratory chain impairment, membrane permeability changes, and Ca^{+2} homeostasis disturbances. These alterations contribute to the mentioned neurodegenerative conditions by exacerbating neuronal dysfunction. In our investigation, oxidative stress induced rat derived NSCs (rNSC) were used to create organoid models by using 3D cell culture techniques. We aimed to evaluate oxidative stress caused by mitochondrial damage in organoid models.

Materials And Methods

This research was performed in line with the principles of the Declaration of Helsinki and was ethically approved by the Non-Interventional Clinical Research Ethics Committee of Kocaeli University, as evidenced by documentation number KÜ GOKAEK-2020/47. rNSCs were sourced from the Cell Collection at the Center for Stem Cell and Gene Therapies Research and Application, Kocaeli University.

rNSC cell culture

In rNSC culture process, the medium used was DMEM F12 supplemented with neural supplement (StemPro; 1X), heparin (0.02%), B27 (1X), glutamax (1%), EGF (epithelial growth factor; 10 ng/ml), FGFb (fibroblast growth factor basic; 20 ng/ml), and penicillin/streptomycin (Gibco; 1%). The medium was replaced every two days until the neurospheres reached an adequate size, at which point they were collected and mechanically dissociated into a single-cell suspension. The single cells were then replanted in culture flasks for subculturing.

Characterization of NSCs

The phenotypes of NSCs were confirmed through microscope examination (Olympus IX71) and their capacity for differentiation was assessed. To promote spontaneous differentiation, the cells were seeded onto surface-coated 6-well plates and cultured in a differentiation medium comprised of DMEM F12 supplemented with N2 supplement (1%), B27 supplement (1%), EGF (10 ng/ml), glutamax (1%), and penicillin/streptomycin antibiotic solution (1%) for a period of one week. The culture medium was replaced every three days.

Immunofluorescent staining

To perform immune staining, the samples were subjected to fixation in 4% paraformaldehyde (PFA) for a period of 15 min, followed by permeabilization with 0.1% Triton X-100. The cells were incubated with Superblock serum for 30 min, and a primer antibody (diluted at a ratio of 1:100) was applied overnight at a temperature of 4 °C. Subsequently, a PBS wash was carried out to remove the primer antibody, and the cells were incubated with secondary antibodies for 90 min. Finally, the slides were mounted using DAPI-containing mounting medium (Santa Cruz Biotechnology). Afterwards, samples were imagined under a lazer scanned confocal microscope (Leica DMI 4000, Germany) (Tokuc et al. 2021). The antibodies utilized for immunofluorescent staining in terms of cell-specific markers were given in Table 1.

Table 1: Primary antibodies utilized for immunofluorescent staining

Antibody	Supplier	Cat. no.
Nestin	Biorbyt	Orb-86833
Glial Fibrillary Acidic Protein (GFAP)	Santa Cruz Biotechnology	Sc-33673
Neural/Glial Antigen (NG2)	Abcam	Ab-50009

S100	Abcam	Ab-868

Examination of gene expression

The acquisition of total RNA was conducted using the High Pure RNA Isolation Kit (Roche Applied Science in Mannheim, Germany) (Oz Oyar et al. 2022). The RNA was extracted from cells by lysing them with lysis buffer, followed by purification through a column, according to manufacturer's guidelines. The synthesis of single-strand cDNA was then carried out using the Transcriptor High Fidelity cDNA Synthesis Kit (Roche Applied Science in Mannheim, Germany). The expression levels of the genes were determined through the use of the LightCycler 480 DNA SYBR Green I Master and gene-specific primers, along with LightCycler 480 real-time PCR instrument from Roche Diagnostics. This process was conducted in accordance with the manufacturer's protocol and utilized primers were given in Table 2.

Table 2: Primers used for rNSC Characterization

Genes	Sequences (5'-3')
Glial Fibrillary Acidic Protein (GFAP)	TCCTGGAACAGCAAAACAAG
	CAGCCTCAGGTTGGTTTCAT
Tyrosine Hydroxylase (TH)	TCGGAAGCTGATTGCAGAGA
	TTCCGCTGTGTATTCCACATG
Nestin	CCCTTAGTCTGGAGGTGGCTA
	GGTGTCTGCAACCGAGAGTT
Beta III Tubulin (TUBB3)	AGAGCCATTCTGGTGGAC
	GCCAGCACCACTCTGACC
Actin Beta (ACTβ)	AGAGAAGCTGTGCTATGTTG
	GTACTCCTGCTTGCTGATCC
Neurofilament Light Polypeptide (NF-L)	TCCAGTTTGTTGATTGTGTCCT
	TGAACGAAGCTCTAGAGAAGCA
Superoxide Dismutase (SOD1)	CGGATGAAGAGAGGCATGTT
	CCACCTTTGCCCAAGTCATCT
Heme Oxygenase (HO1)	GGTGTCCAGGGAAGGCTTTAAG
	GTGCAGCTCCTCAGGGAAGTAG
Ki-67	GCAGACAAGCCTTCAGCAGTAA
	TGGTACCATTGTCATCAATTTCAGT
Brain Derived Neurotrophic Factor (BDNF)	GTCCCTTCTACACTTACCTCTTG
	CTTTGTTTCACCCTTTCCACTCCT

Ciliary Neurotrophic Factor (CNTF)	CACCCCAACTGAAGGTGACT
	ACCTTCAAGCCCCATAGCTT

Hydrogen peroxide treatment on NSCs

NSCs were subjected to preconditioning by exposing them to varying concentrations of hydrogen peroxide. Initially, the cells were single cell suspended and seeded onto 96 well plates. Thereafter, a medium containing hydrogen peroxide at concentrations ranging from 5 µM to 150 µM was added onto the cells, and a 30-min incubation was performed at 37 °C. Following the incubation, the medium containing hydrogen peroxide was replaced with the standard culture medium.

Determination of appropriate hydrogen peroxide concentration

Cell viability assay

The process of cell plating was executed at a concentration of 10,000 cells per well in a 96-well plate using a medium containing hydrogen peroxide. The plate was then incubated for 30 min at a temperature of 37 °C. The medium was then replaced with standard culture medium, and the cells were cultured for 24 h. The cell viability was assessed using a WST-1 kit (Roche Diagnostics, Québec, Canada). To accomplish this objective, 10 µl of the WST-1 cell proliferation and viability assessment solution were added to the cells in the 96-well plates that were cultured. The cells were then incubated for 2 h at a temperature of 37 °C. The absorbance data were acquired using a spectrophotometer (Molecular Devices, VersaMax) with a wavelength of 450 nanometers.

β-Galactosidase (β-Gal) staining and spectrophotometric analysis

In order to evaluate the impact of hydrogen peroxide concentrations on β-galactosidase staining, a 96-well plate was utilized. Each well contained 10,000 cells and was seeded with hydrogen peroxide-containing medium. The cells were then incubated at 37°C for 30 min, followed by the addition of standard culture medium to wells. The cells were cultured for 24 h at 37°C, after which a histochemical analysis was conducted using the Senescence Cells Histochemical Staining Kit (Sigma). The purpose of this analysis was to determine effects of various hydrogen peroxide concentrations on the cells. Briefly, cells were collected and suspended in a medium, which was then centrifuged in a cytocentrifuge (Hettich ROTOFIX 32) to adhere them to slide surface. The cells were then fixed with a 1X fixation solution. Subsequently, the samples were incubated overnight at 37°C with a staining solution to provide visual data for choosing optimal concentration of hydrogen peroxide. Additionally, to evaluate β-Gal activity associated with cell senescence, the cells were fixed in a 1X fixation solution for 15 min at room temperature and incubated overnight at 37°C (without CO2) with staining solution. The absorbance data were collected by a spectrophotometer at 400 nm (Molecular Devices, VersaMax).

TMRM staining for detection of changes in mitochondrial membrane potential

Mitochondrial membrane potential were assessed using a TMRM staining solution (Thermo Scientific, Cat no: M200360). Basically cells were plated at determined density in a 96 well culture plate with hydrogen peroxide containing medium and incubated for 30 min in a 37 °C. After that medium replaced with the standard

medium and cells cultured for 24 h at 37 °C. After that cell containing medium was collected with centrifuge excess medium removed and cells stained with TMRM dye for 30 min in a 37 °C. The changes in Mitochondrial membrane potential were evaluated with flow cytometer analysis.

Generation of organoids with stress induced NSCs

NSCs preconditioned with 75 µM hydrogen peroxide for 30 min were mixed with 10 µL matrigel (Matrigel Matrix Growth Factor Reduced, BD) per well and plated to a non-adhesive 96-well plate. Incubation was carried out at 37 °C for 2 h. At the end of the time, 100 µL of differentiation medium was added to the wells in order to remove the matrigen droplets from the bottom and start the culture. Organoids were cultured in non-adhesive 96-well plate for 28 days. During this period, ectodermal differentiation was induced by B27 in cells. The medium was consistently altered every three days in experimental set-ups.

Characterization of an in vitro 3D NSC organoid model

Cryosectioning

Organoids were harvested at 14th day and 28th day to perform immunocytochemistry analyses, for this purpose samples washed two times with phosphate-buffered saline (PBS; Sigma-Aldrich) and fixation was performed with 4% PFA for 15 min. Samples were washed with PBS one more time to eliminate fixative and placed in 30% sucrose overnight at 4 °C. After taht to kept organoids more stabile for sectioning embedding solution with 7.5% gelatin and 10% sucrose was added to the organoids and kept at 37 °C for 20 min. Samples were taken into metal cassettes and fast freezing was performed by keeping them on the mixture prepared with dry ice and 100% alcohol for 1-2 min. Organoids were sliced 15 µm thickness by using a cryostat, LEICA CM1520 (Leica Biosystems, Wetzlar, Germany, http://www2.leicabiosystems.com). Cryosections were mounted on positive charged slides and stored at 20°C.

Hematoxylin and eosin staining

Prior to staining, sections were rehydrated with decreasing alcohol series for 4 min each. Sections were placed in haematoxylin solution for 5 min and washed in tap water for 4 min. After that sections were placed in bluing solution for 15 s and stained with eosin solution for up to 3 min. Finally sections were dehydrated by increasing ethanol series and mounted using Entellan (Sigma Aldrich Cat no: 107961). Gross images were obtained by using Leica DMI 4000 microscope (Leica Biosystems, Wetzlar, Germany, http://www2.leicabiosystems.com) (Ergen at al. 2022).

Immunofluorescent staining

Slides were placed in 96% ethanol for 20 min. Sections were then taken into 50 Mm pH 6.0 citrate solution and microwave irradiated antigen retrieval procedure was performed for 20 min. Slides were permeabilized in 0.1% Triton-X up to 7 min and blocked with protein block solution (Abcam Cat no: ab64226) for 10 min. Sections were incubated with primary antibodies diluted in antibody diluent solution (Invitrogen Ref no: 003118) at 4°C overnight. Slides were washed three times with PBS-T for 10 min each and incubated with secondary antibody for 90 min at 37°C. After that samples were washed with PBS-T and mounted with DAPI containing mounting

medium (Santa Cruz Biotechnology). Afterwards, samples were imagined under a lazer scanned confocal microscope (Leica DMI 4000, Germany). The cell-specific markers used for organoid characterization given in Table 3.

Table 3: Primer antibodies used in immune staining for organoid charazterization

Antibody	Supplier	Cat. no.
Beta III Tubulin (TUBB3)	Biorbyt	Orb-100281
S100	Abcam	Ab-868
Neural/Glial Antigen (NG2)	Abcam	Ab-50009
Microtubule Associated Protein (MAP2)	Abcam	Ab-11267
Tau	Abcam	Ab-131354
Glial Fibrillary Acidic Protein (GFAP)	Santa Cruz Biotechnology	Sc-33673
Tyrosine Hydroxylase (TH)	Santa Cruz Biotechnology	Sc-73152

Organoid β-Galactosidase staining

Organoids were subjected to a 1X fixation solution for a period of 20 min at room temperature. Following this, the organoids were washed with PBS three times for a duration of 10 min each. Afterwards, the organoids were incubated overnight at 37 °C without CO_2 using fresh senescence-associated β-Gal staining solution. The following day, microscopic imaging was conducted, and the organoids were disintegrated using mammalian extraction buffer (M-PER, Thermo Scientific). Finally, absorbance readings were obtained using a spectrophotometer (Molecular Devices, VersaMax) at 400 nm.

Superoxide dismutase (SOD) analysis

SOD enzyme activity was analyzed by using a SOD analysis kit (EnzyChrom Superoxide Dismutase Assay Kit, BioAssay Systems). The organoids were taken into Eppendorf, 100 µl PBS was added and the integrity of the structure was disrupted with an insulin injector to obtain a cell suspension. Samples were added to 96 well as 20 µl per well. Next a working solution containing WST-1 and Xanthine enzyme was added on samples and reaction was started by adding Xanthine oxidase enzyme on the samples. SOD enzyme activity was analyzed by making spectrophotometric measurements at 400 nm wavelength at 0 and 60 min.

Tetramethylrhodamine methyl ester (TMRM) staining of organoid

Prior to staining, cryosections were brought to room temperature and rehydrated with decreasing alcohol series for 4 min each. 10 μM TMRM containing dye solution was added to the samples and staining was carried out at 37 °C for 30 min. To obtaine visual datas, excess dye was removed and slides were mounted with DAPI containing mounting medium (Santa Cruz Biotechnology).

Quantification of total mitochondria by mitotracker red staining

Mitotracker red is a fluorescent dye that shows deposition in the mitochondrial membrane by binding to thiol-reactive chloromethyl groups. Prior to staining, cryosections taken to the room temperature and rehydrated with decreasing alcohol series for 4 min each. 500 nM mitotracker red (Thermo Scientific Cat no: M22425) containing dye solution was added to the samples and staining was carried out at 37 °C for 30 min. At the end of the period, the dye was removed and slides were mounted with DAPI (Santa Cruz Biotechnology) and made ready for analysis. Afterwards, samples were imagined under a lazer scanned confocal microscope (Leica DMI 4000, Germany).

Gene expression analysis

The RNA extraction process was carried out using the QIAGEN RNeasy Mini kit for the 1st, 14th, and 28th day organoid models. The organoids were broken down using the lysis buffer provided in the kit, and then the RNA was isolated using column purification, as per the manufacturer's instructions. The Transcriptor High Fidelity cDNA Synthesis Kit (Thermo Scientific) was used to synthesize single-strand cDNA, and the LightCycler 480 DNA SYBR GreenI Master from Roche Applied Science along with gene-specific primers on a LightCycler 480 real-time PCR instrument from Roche Diagnostics was used to determine gene expression levels. The process was carried out according to the manufacturer's protocol, and the gene-specific primers used were given in Table 4.

Table 4: Primers used in RT-PCR for organoid characterization

Gene	Sequences (5'-3')
NADPH Oxidase 4 (NOX4)	AGCAGAGCCTCAGCATCTGTTCTT
	TGGTTCTCCTGCTTGGAACCTTCT
P22PHOX	AAAGAGGAAAAAGGGCTCCA
	TAGGCTCAATGGGAGTCCAC
Neurotrophic Factor (NRF2)	AGAGCCATTCTGGTGGAC
	GCCAGCACCACTCTGACC
RAGE	CTACCTATTCCTGCAGCTTC
	CTGATGTTGACAGGAGGGCTTTCC
Dual Oxidase 1 (DUOX1)	AGTTCCTGGACATCCTGGTG
	GTCAGCTCCTCCTTGTCCTG

Superoxide Dismutase (SOD1)	CGGATGAAGAGAGGCATGTT
	CCACCTTTGCCCAAGTCATCT
Heme Oxygenase (HO1)	GGTGTCCAGGGAAGGCTTTAAG
	GTGCAGCTCCTCAGGGAAGTAG
Monocarboxylate transporter 4 (MCT4)	CTTGCTCCTTTAGCCACCAC
	GAAACTGGCAAGTCCCAAAA
Indian Hedgehog (IHH)	TGACAGAGATGGCCATCTC
	AAACTCGCGCCTCTTGCCTA
Sonic Hedgehog (SHH)	TTTCACAGAGCAGCAGTGGATGC
	TTAAATGCCTTGGCCATCTC
Notch 1	CTCTACAGGCACACTCGTAGC
	AACGCCTACCTCTGCTTCTG
Actin Beta (ACTβ)	AGAGAAGCTGTGCTATGTTG
	GTACTCCTGCTTGCTGATCC
Nucleotide-binding oligomerization domain-containing protein 2 (NOD2)	TTCTGCCTTACGAGGGTTACTCTCT
	ATGGTCCTCAGCTTAGCAGTGAAC
WNT3A	GTGAAGACATGCTGGTGGTC
	GGGCACCTTGAAGTAGGTGT
Noggin (NOG)	TGTGGTCACAGACCTTCTGC
	GTGAGGTGCACAGACTTGGA

Determination of total protein in organoids with bicinchoninic acid (BCA) method

Total protein concentration in the organoid models were analyzed by using the BCA Analysis Kit (SMART BCA Protein Assay Kit). First organoids were taken into eppendorf, 100 µl PBS was added and the integrity of the structure was disrupted with an insulin injector to obtain a cell suspension. Samples were added to 96 well as 25 µl per well. Then bicinchoninic asid containing working solution was added and incubation was performed at 37 °C for 30 min. The analysis was carried out by making spectrophotometric measurements at a wavelength of 562 nm.

Statistical analysis

The IBM SPSS 20.0 software package (SPSS Inc., Chicago, IL, USA) was utilized to conduct a statistical analysis. The Normal distribution was assessed using the Kolmogorov-Smirnov test. Numerical variables that followed a normal distribution were reported as the mean ± standard deviation, while those that did not were reported as the median (25^{th} percentile-75^{th} percentile). A one-way analysis of variance (ANOVA) was used to determine differences between groups for numerical variables following a normal distribution. A p-value of less than 0.05 was considered statistically significant (Tekin et al. 2024; Furat Rencber et al. 2018; Rende et al. 2024).

Results

Characterization of rNSC

NSC's were exhibited neurosphere structures, which are characteristic features of NSCs and they maintained their phenotype during serial passages. The cells differentiated into neuron, astrocyte and oligodendrocyte after 7 days of culture. The formation of the neurosphere structures and generation of several cell types indicated that this cells possessed the NSC character.

Fig. 1. Characterization of rNSC. NSCs were analyzed by bright field microscopy (a). The differentiation capacity of rNSC's into neural (e) and glial cell lines (a, c, d) were determined with immune staining. The nuclei were stained with DAPI (blue b-e). Scale bar: 50, 100, and 200 μm.

Determination of appropriate hydrogen peroxide concentration

The optimum H_2O_2 dose for preconditioning cell to oxidative stress was determined as a 75 μM H_2O_2. To determine optimum H_2O_2 dose WST-1 assay, SA-β-gal Staining and RT-PCR analyses were performed. For WST-1 assay briefly, NSCs were treated for 30 min with H_2O_2 at concentrations ranging from 5 μM to 150 μM. As a result low and high dose H_2O_2 caused cell death (5μM, 150μM). β-gal staining was performed for all hydrogen peroxide doses and intensifying staining was observed at increasing concentration values. 75 μM H_2O_2 dose showed intense staining compared to other doses. Results obtained from β-gal staining indicated that H_2O_2 concentrations above 75 μM caused lethal effect on cells. The expression pattern of differentiation markers, oxidative stress markers, cell survival markers and proliferation marker was analyzed with real time PCR (Fig. 2). The expression of differentiation markers increased at 10 μM H_2O_2 concentration, decreased at 20 μM and then exhibited a secondary increase profile at 75 μM and 100 μM. Oxidative stress related markers showed similar expression profile with differentiation markers which expressions increased 10 μM H_2O_2 concentration, decreased at 20 μM and then exhibited a secondary increase profile at 75 μM and 100 μM. When expression levels of BDNF and CNTF were examined, 10 μM H_2O_2 caused a great amount a stress in cell and there was an increased expression of cell survival genes associated with stress. The expression level of these markers decreased at 20 μM H_2O_2 concentration and increased again for 50 and 75 μM H_2O_2 concentrations. The expression pattern of profilferation marker increased at 10 μM H_2O_2 concentration, decreased at 20 μM and then exhibited a secondaty increase profile at 75 μM H_2O_2 concentration. The results showed that 75 μM H_2O_2 concentration was appropriate value for preconditioning studies.

(a)

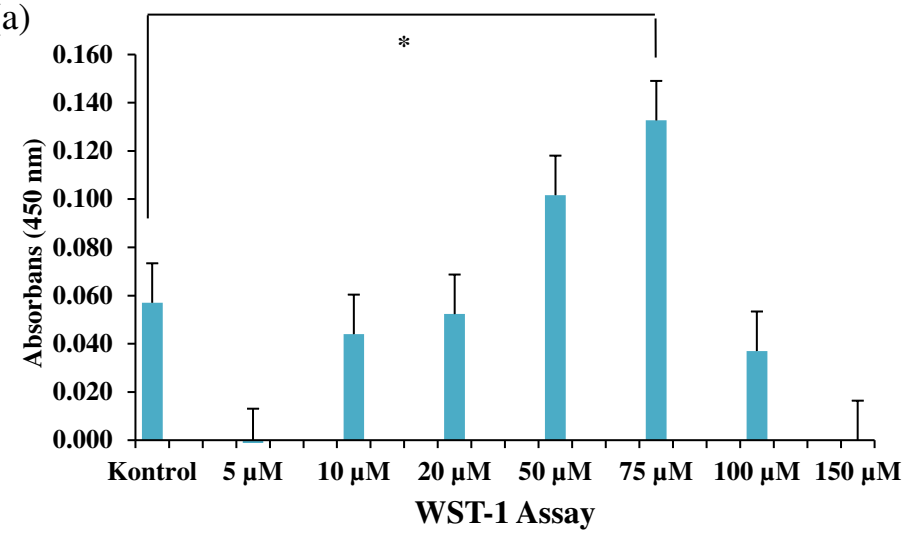
*
0.160
0.140
0.120
0.100
0.080
0.060
0.040
0.020
0.000
Absorbans (450 nm)
Kontrol
5 µM
10 µM
20 µM
50 µM
75 µM
100 µM
150 µM
WST-1 Assay

(b)

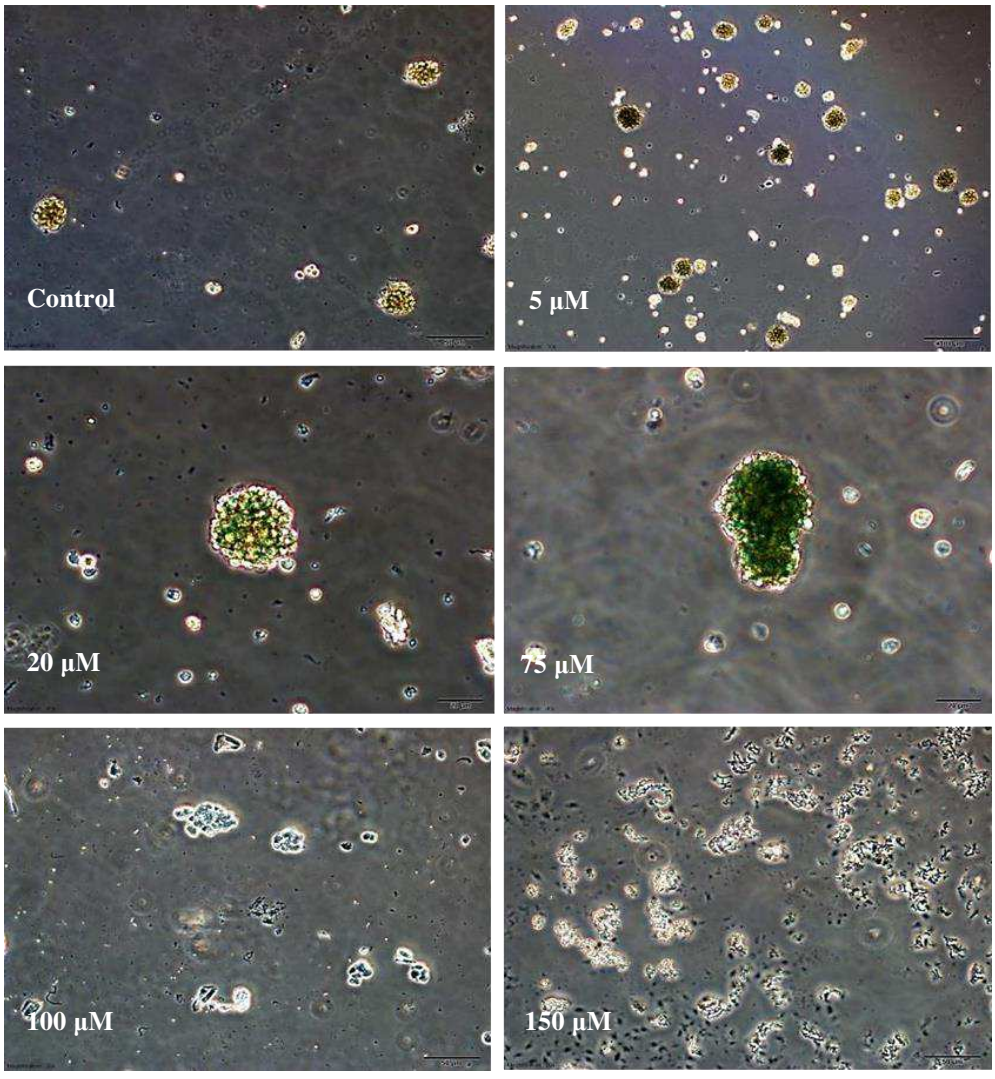
Control
5 µM
20 µM
75 µM
100 µM
150 µM

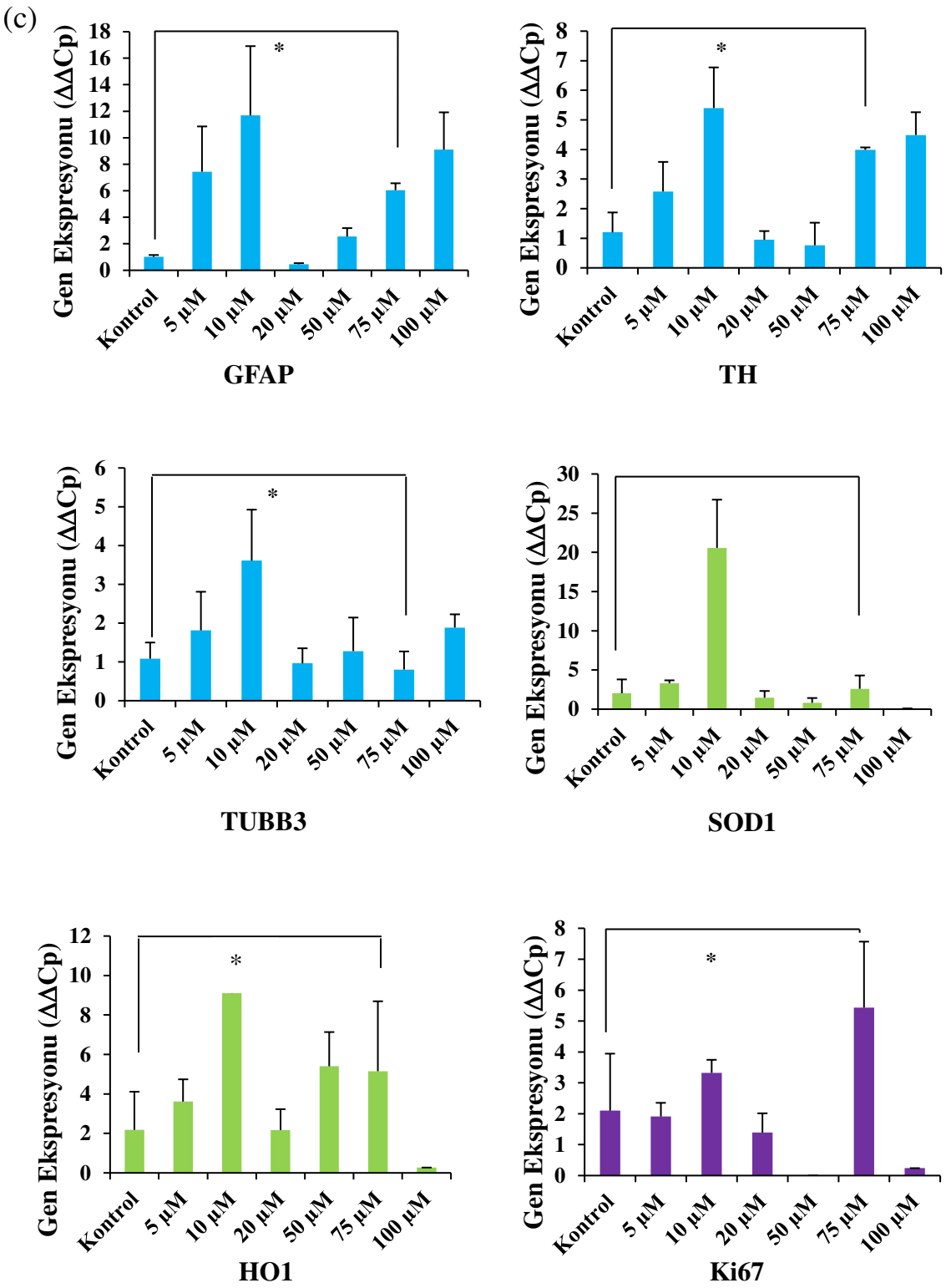

Fig. 2. Determination of appropriate H_2O_2 concentration for oxidative stress induction. WST-1 assay performed after 30 min of H_2O_2 application to rNSC's at varying concentration values (a). Beta galactosidase staining to sNKHs after 30 min of H_2O_2 application at varying concentration values, Scale bar: 50 µm (b). Differentiation, oxidative stress, cell survival and proliferation gene expressions (c). (*: $p < 0.05$).

Formation of organoids created with stress induced NSCs

This protocol outlines the generation of 3D cerebral organoid formation from rNSC's and their following analysis. These method is easy to perform in a standart tissue culture systems using basic equipments. Furthermore, organoids can be examined at various timepoints to study a variety of developmental stages. Begining of this protocol first cells were preconditioned with 75 µM H_2O_2. After that cells were mixed with growth factor reduced matrigel and cultured in non adhesive 96 well culture dish. Organoids were cultured in standart culture conditions up to 28 day. During this period, ectodermal differentiation was induced by B27 supplement.

NSCs was quickly expanded their number once placed in Matrigel and by the time 9-16 the entire organoid was diffucult to examine with standart tissue-culture microscope. Organoids were systematically examined during the culture. In early stages of culture, cells in the control organoid model showed a tendency to form clusters. But there is no such a thing was observed organoids who created with preconditioned cells.

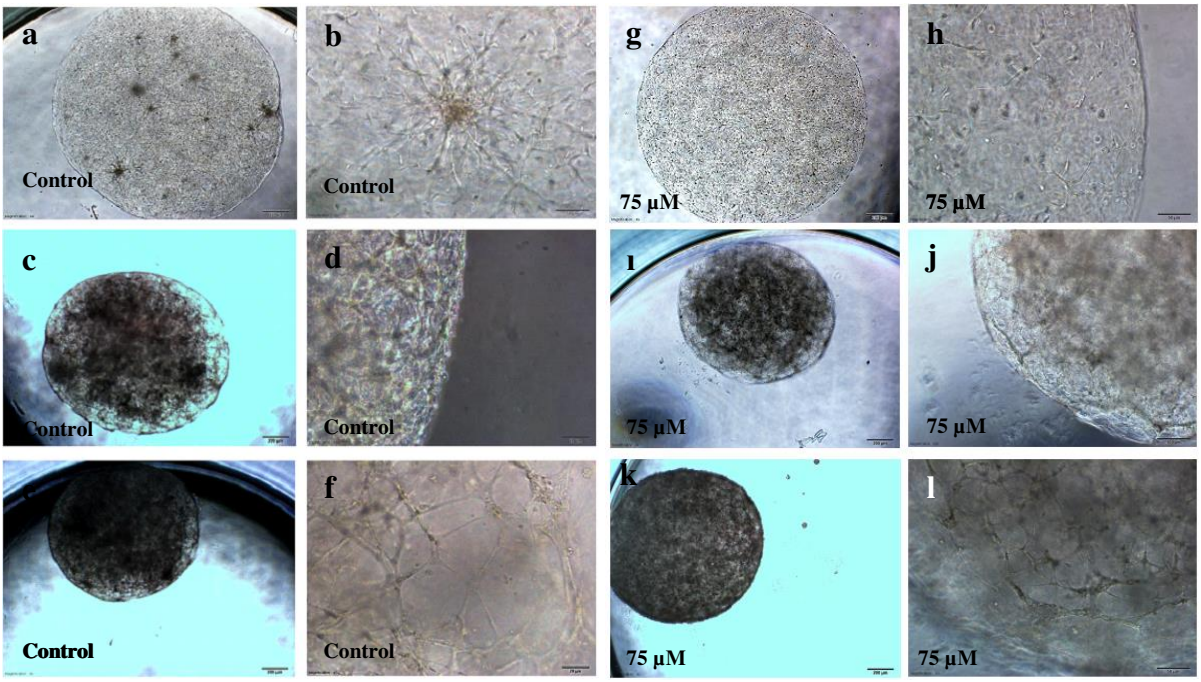

Fig. 3. rNSC organoid models in culture. 1st day in culture (a, b), 14th day in culture (c, d), 28th day in culture (e, f). 1st day in culture (g, h), 14th day in culture (ı, j), 28th day in culture (k, l). Scale Bar: 50, 100, and 200 µm.

Histological and cytological analysis of NSC organoid

Organoids were created by using oxidative stress induced rNSC cells and cultured in differentiation medium. During the culture period it was seen that surface structures on the organoids occured between D9 and D10. Histologic exemination of organoids revealed a spesific cellular dispersion and neuroepithelial structures consist with the develoment of organoids. When immunofluorescent stains have been used to further evaluate organoid models at 14th day, it was seen that most of cells in organoids were positive for β3-tubulin, MAP2 and NG-2 consist with neural differentiation. Moreover, many of the cells in organoids were also positive for Tau marker.

Additional experiments were carried out on 28th day organoid models. 28th day organoids showed some simillarity to those at 14th day, but tented to be larger and these often showed increased complexity and in 28th day organoids cells showed additional positivity for GFAP, S100. Furthermore, in both 14th day and 28th day organoids were negative for tyrosine hydroxylase.

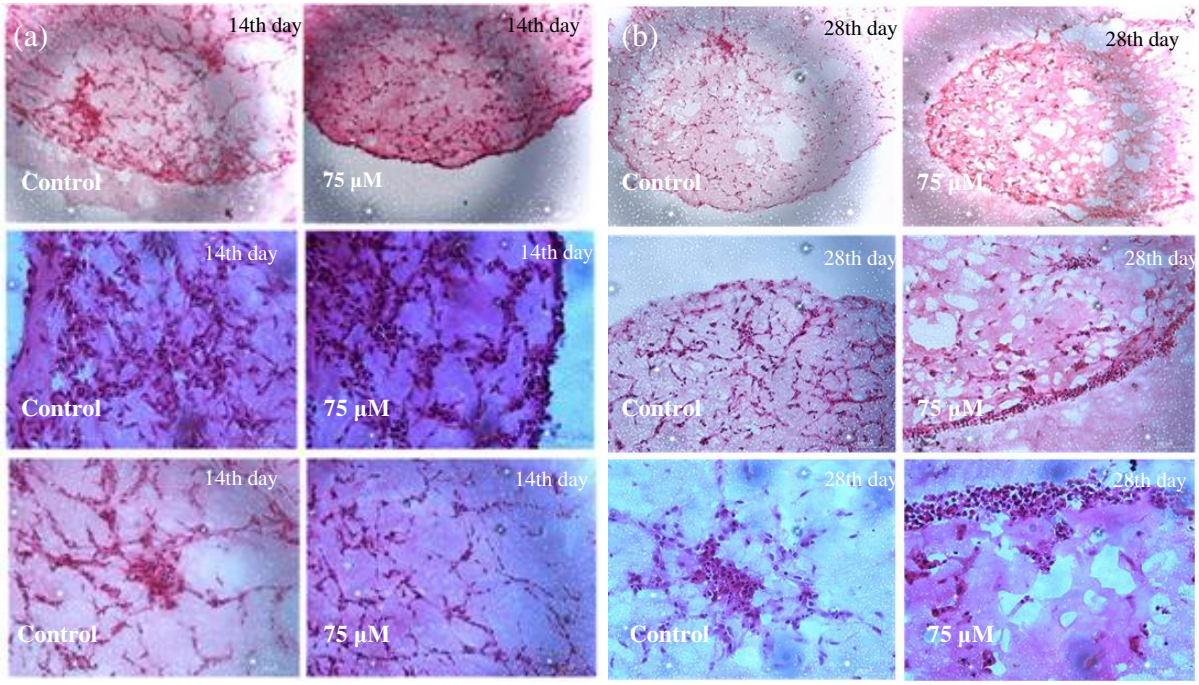

(c)

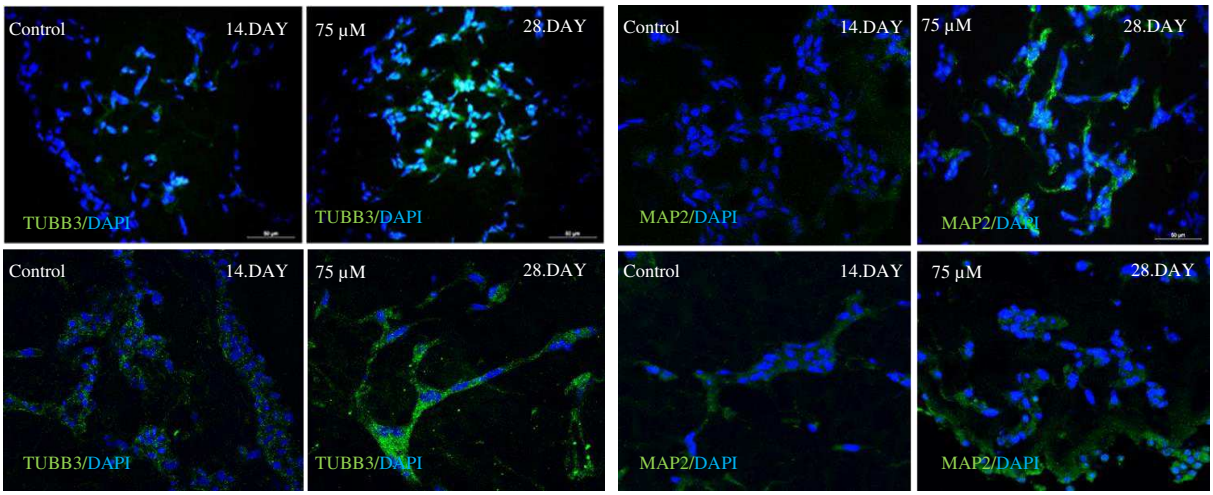

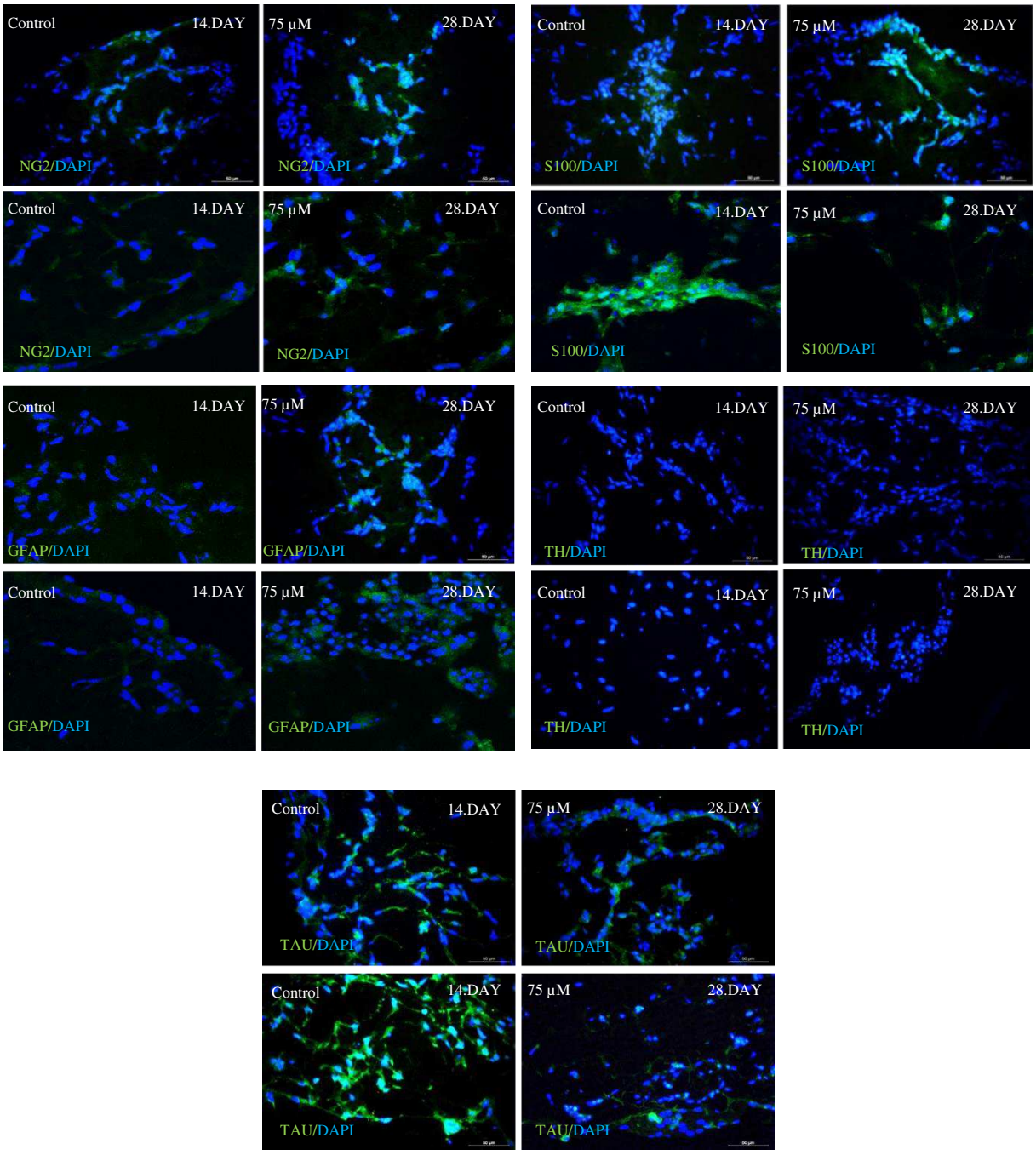

Fig. 4. Morphologies of the control and oxidative stress organoid models. 14th day organoid models hematoxylin and eosin staining (a). 28th day organoid models hematocylin and eosin staining (b). Characterization of control and oxidative stress organoid models with immune staining (c). Scale bar: 50, 100, and 200 µm.

Gene expression in NSC organoids

To further characterize organoids, expression of various markers such as oxidative stress, autophagy and apoptosis, cell survival in 1st day, 14th day and 28th day organoids created with oxidative stress induced NSCs. Differentiation markers (SHH, IHH and Wnt-3a) analysis showed significantly increased expression in 28th day organoids. Oxidative stress markers (SOD1, HO1, DUOX1 and MCT-4) combined analysis indicated that significant over expression profile at 14th day and 28th day time points for HO1. SOD1 oxidative stress marker

showed increased expression only 14th day, for DUOX1 marker incerased expression profile seen only in 28th day. To analyse mitochondrial biogenesis and mitochondrial ROS homeostasis MCT-4 and NRF2 markers were used. NRF2 expression showed significant increased expression at 28th day. Besides MCT-4 expression showed increased expression both time points. NOD2 marker, which is involved in autophagy and apoptosis, supports cellular survival and provides the expression of antiapoptotic proteins. NOD2 expresison showed significant increased expression at 28th day. NOX4 one of the NOX family subunits, function as oxygen sensors and catalyze the reduction of oxygen to various ROS. NOX4 expression analysis showed significant decreased expression at 14th day time point.

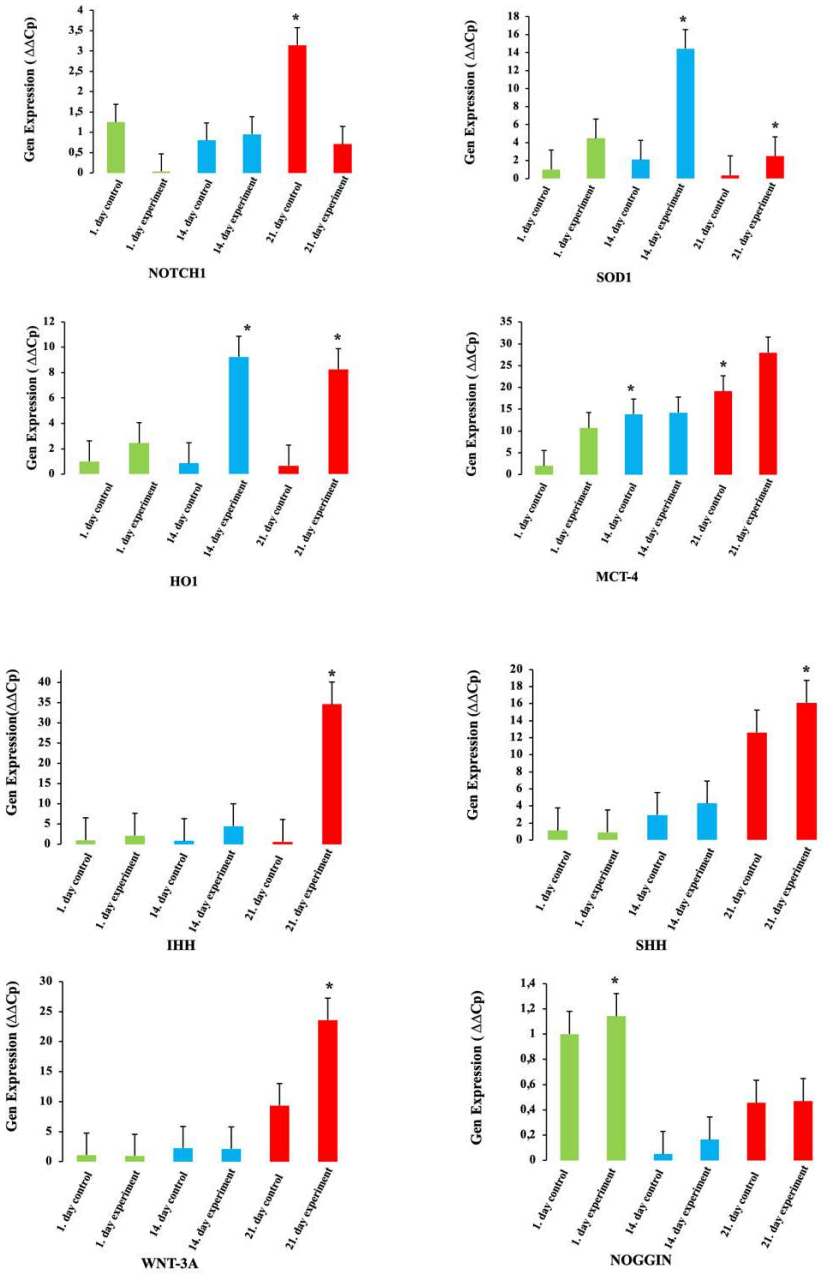

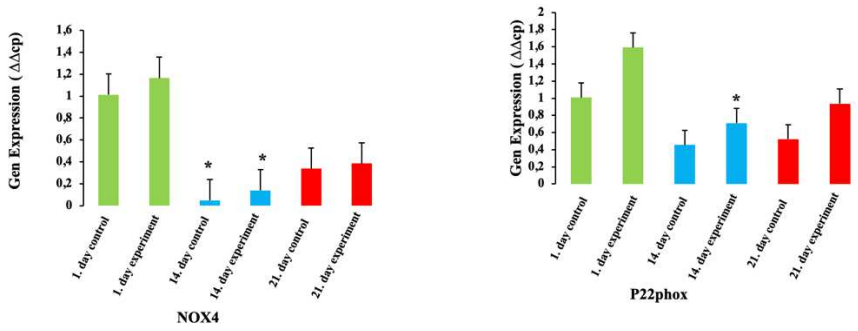

Fig. 5. The evaluation of gene expression of control and oxidative stress organoid models. β-Actin was used as the reference gene (*: $p < 0.05$).

Detection of oxidative stress in organoid models by SOD analysis

In order to reveal the SOD activity in the organoid models, briefly organoids were collected on the 1st, 14th and 28th days of the culture and level of SOD in the models were analyzed using the SOD analysis kit (EnzyChrom Superoxide Dismutase Assay Kit). As a result, in 1st day organoids it was determined that oxidative stress-induced SOD activity was high in organoids created with H_2O_2 applied cells, and SOD activity was not observed in the organoid model created with healthy cells (Fig. 6). In the organoid models on the 14th day, a necrotic region was occured due to cellular localization in the control group model, resulting increase in SOD activity compared to the 1st day. It was determined that the SOD activity of the H_2O_2 applied model increased compared to the 1st day and the SOD activity of this group was higher then the control group (Fig. 6). In the 28th day organoid models, there was a decrease in SOD activity in both groups. It was determined that the SOD activity of the control group was above the SOD level of the organoid model of the experimental group, the reason of this the increase in the oxygen-free zone created by the cells located in the center of the model (Fig. 6).

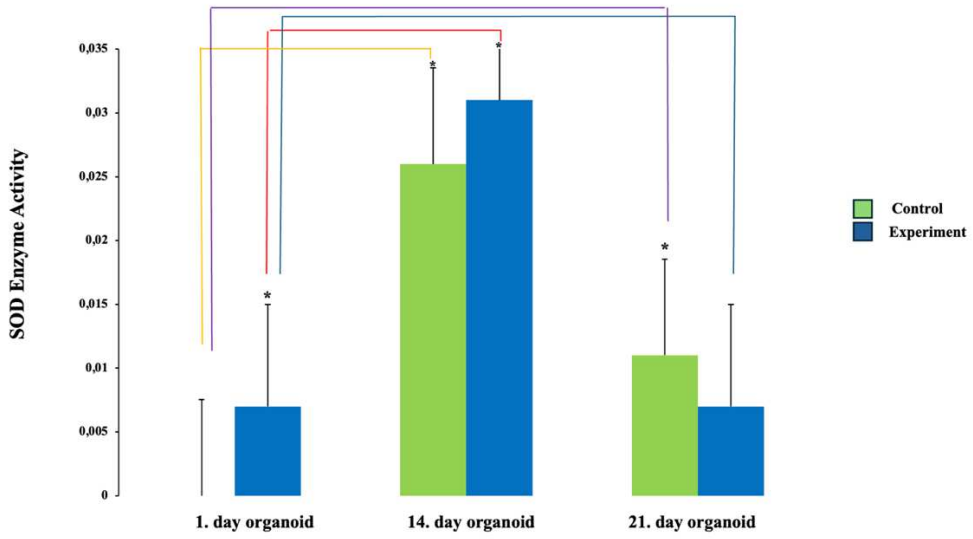

Fig. 6. 1st, 14th, and 28th day SOD activity of control and oxidative stress organoid models (*: $p < 0.05$).

BCA assay in NSC organoids

BCA analysis was implemented to reveal total protein concentrations in the organoid models. As a result of the BCA analysis, the protein amount of the organoids formed by the cells treated with H_2O_2 increased by 5.03% compared to the organoid model of the control group. Likewise, when the organoid models on the 14th day were compared with the control organoid model on the 1st day, the protein amount of the organoid model formed by the cells treated with H_2O_2 an increase by 43.66% (Fig. 7).

It was observed that there was a 52.25% decrease in total protein amount in the 28th day control organoid model compared to the 1st day organoid. It was observed that the amount of protein in the 28th day H_2O_2 organoid model decreased by 85% compared to the 14th day H_2O_2 organoid model, because of the decrease in the effect of oxidative stress-induced stimulation (Fig. 7).

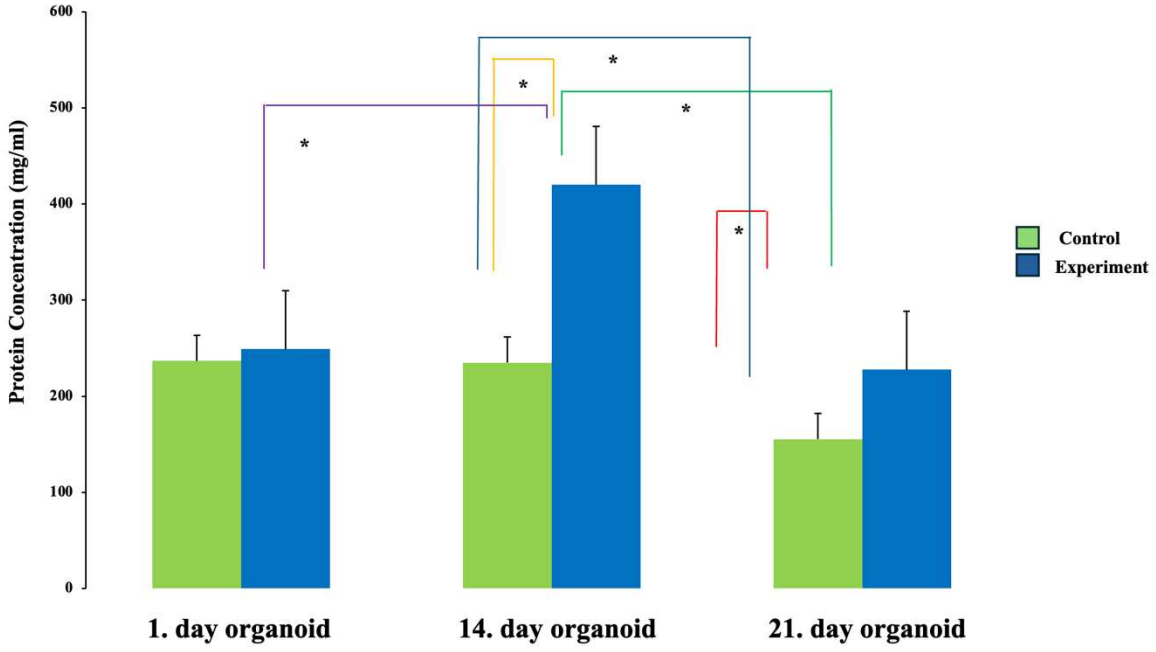

Fig. 7. 1st, 14th, and 28th day BCA analysis of control and oxidative stress organoid models (*: p <0.05).

Mitochondrial Membrane Potential Measurement

TMRM staining

Cationic fluorescent dye tetramethylrhodamine methyl ester (TMRM) staining was performed to detect the mitochondrial membrane potential change in the organoids. When TMRM staining of the 1st day organoid models was examined, it was observed that the staining was weaker in the experimental group compared to the control. TMRM staining of organoid models on the 14th day was similar among the groups. When the TMRM staining of the control and experimental group organoids on the 28th day was examined, it was observed that the sections taken from the experimental group organoids treated with H_2O_2 were stained more intensely compared with control group (Fig. 8).

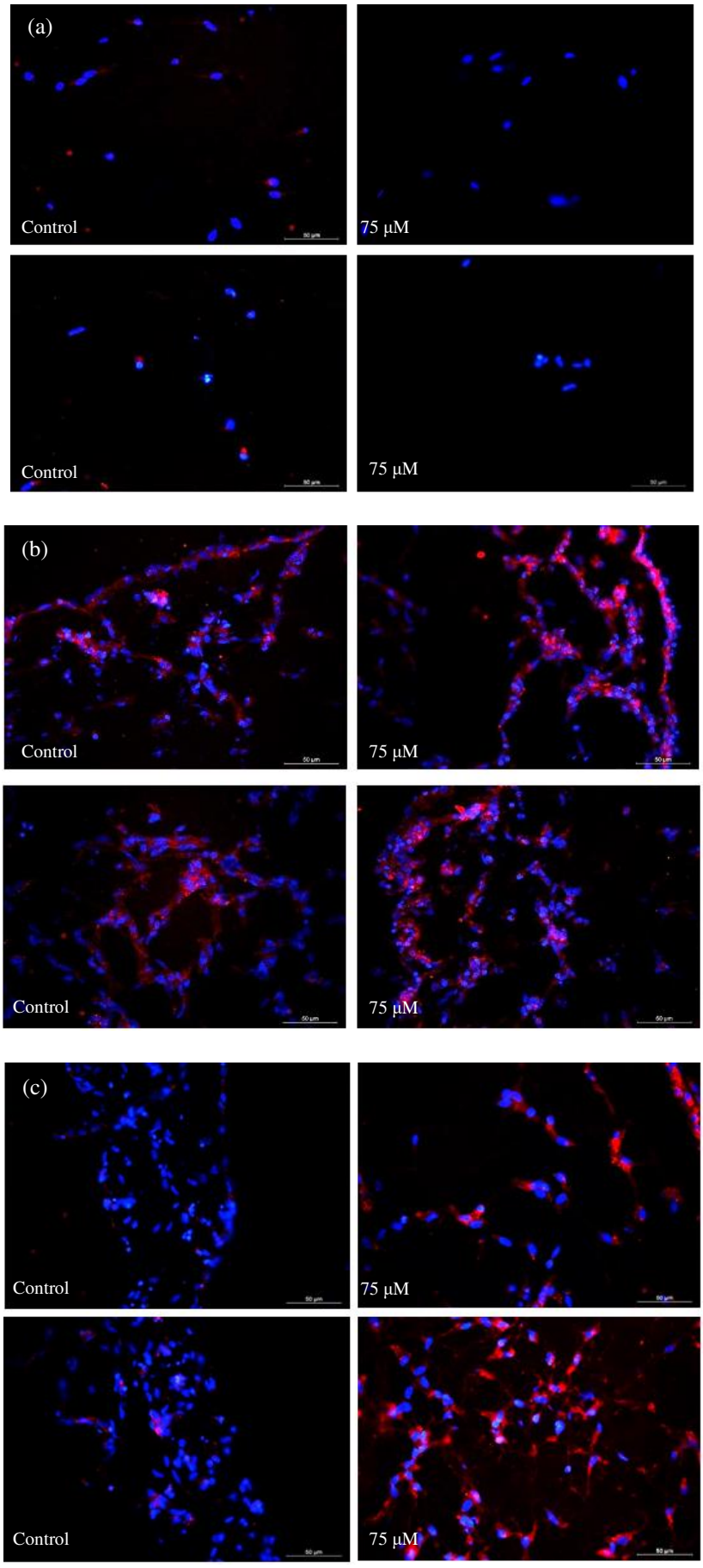
(a)
Control
75 µM
Control
75 µM
(b)
Control
75 µM
Control
75 µM
(c)
Control
75 µM
Control
75 µM

Fig. 8. 1st, 14th, and 28th day control and oxidative stress organoid models TMRM staining. 1st day organoid models TMRM staining (a). 14th day organoid models TMRM staining (b). 28th day organoid models TMRM staining (c). Scale bar: 50 μm.

Mitotracker red staining

To assess the total number of the mitochondria, mitotracker red staining was performed. 1st day control organoid models showed strong positivity compered to model using oxidative stress-treated cells. 14th day organoid models showed similar level of mitotracker staining. When looking at the mitotracker staining in the organoid models on the 28th day, it was seen that the organoids created by using cells exposed to H_2O_2 was more intensely stained with the dye that stains the mitochondria in the cell compared to the control group (Fig. 9).

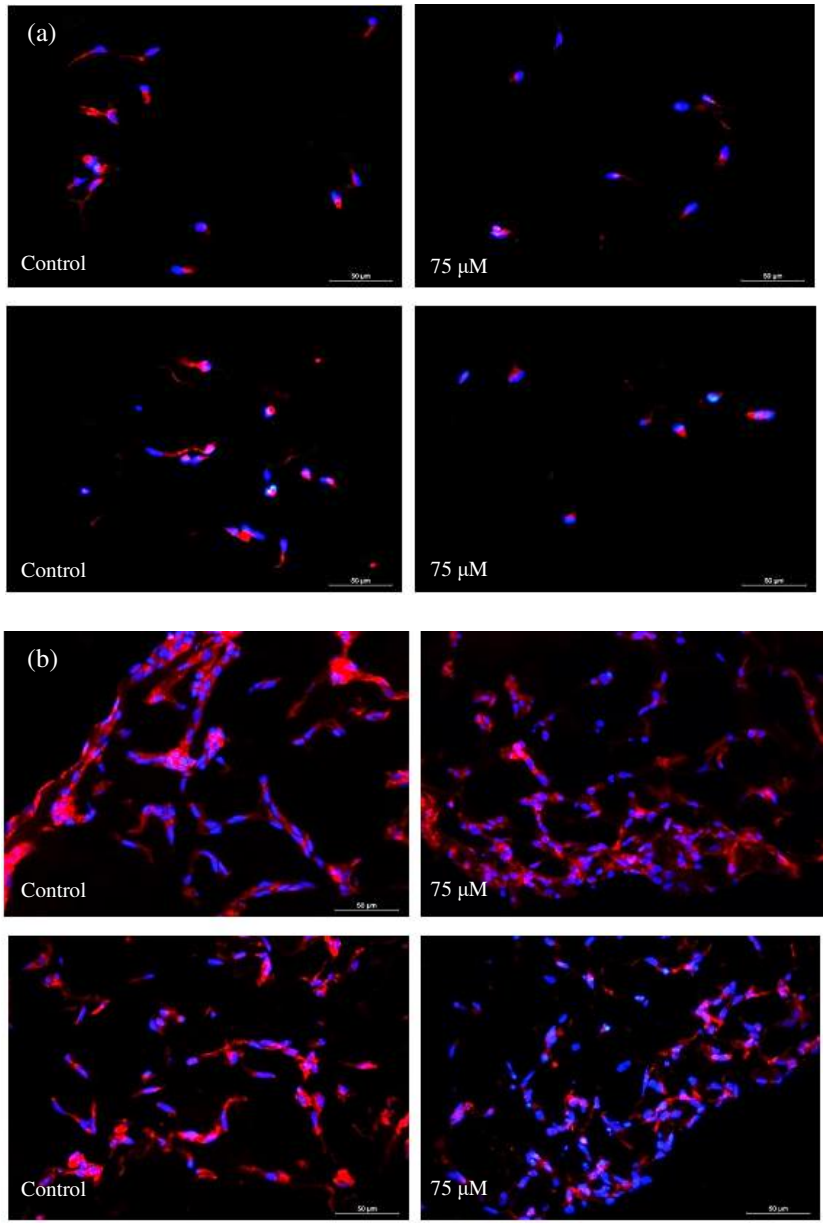

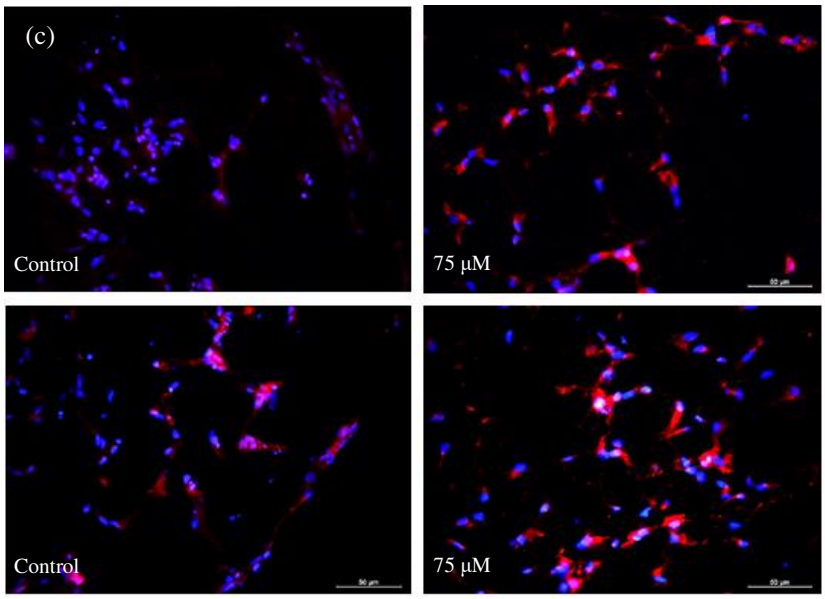

Fig. 9. 1st, 14th, and 28th day control and oxidative stress organoid models mitotracker red staining. 1st day organoid models mitotracker red staining (a). 14th day organoid models mitotracker red staining (b). 28th day organoid models mitotracker red staining (c). Scale bar: 50 μm.

Discussion

Aging has a significant impact on the development of neurodegenerative diseases, which are caused not only by mutations at the gene level but also by changes in cellular compartments. One of these compartments is mitochondria, which play a crucial role in energy metabolism within cells. Abnormal mitochondrial DNA and gene expression patterns have been linked to neurodegenerative diseases. Although there are theories on aging at the cellular level, there is little known about how microscopic failures lead to tissue and organ dysfunction and ultimately affect the entire organism. It is crucial to recognize that interdependence between cells plays a significant role in tissue death. Contrary to what 2D cell cultures suggest, it is not only the cells but the entire tissue that ages under physiological conditions. To better understand the complexity of tissue aging, organoid cultures can be used. These cultures are created by spontaneous growth of high-potency cells on an appropriate support matrix structure, and they mimic in vivo physiological structures in in vitro conditions. Organoid cultures can reveal critical cell-cell and cell-matrix interactions that 2D cell culture techniques fail to predict. Tissue engineering and organnoid technologies hold promise for understanding the development of neurodegenerative diseases as well as other diseases.

Our study aimed to determine the optimal dosage that would induce stress in NSCs. The effects of preconditioning increased in a dose-dependent manner up to a specific threshold, beyond which they decreased, possibly due to the depletion of the cells' intrinsic cytoprotective capacity. NSCs possess a sophisticated antioxidant defense system that regulates reactive oxygen species. These cells have enzymatic defenses against H_2O_2, such as catalase and glutathione peroxidase (Simonian and Coyle, 1996), which are upregulated when cells are exposed to low concentrations of H_2O_2, making them more susceptible to subsequent cytotoxic doses (Valen et al. 1998; Lee and Um 1999; Tang et al. 2007; Sharma et al. 2008). However, under oxidative stress conditions, the cellular antioxidant defense system may become compromised (Conklin, 2000). The accumulation of free

radicals can overwhelm these mechanisms, rendering cells more susceptible to lipid peroxidation, DNA, and protein damage (Berlett and Stadtman, 1997; Cadet et al. 2001). For example, studies have shown that an excess of H_2O_2 can reduce glutathione (GSH) activity (Su et al. 1999; Spector et al., 2002; Hammerschmidt and Wahn, 2004). Based on the analysis of WST-1, it was found that 75 μM of H_2O_2 concentration is the optimal level for achieving the desired outcome in cells. It is worth noting that 100 μM of H_2O_2 concentration is commonly used in studies, as reported in the literature (Konyalioglu et al. 2013; Abdanipour et al., 2018). However, it should be mentioned that using 100 μM of H_2O_2 concentration may cause a decrease in cell viability over time, as previously reported in the literature (Konyalioglu et al. 2013). To exhibit the alteration in the mitochondrial membrane potential brought on by oxidative stress, cells were reared with 75 μM H_2O_2 and stained with the TMRM dye. Consequently of the flow cytometric investigation, it was disclosed that the cells of the control group were more dyed with TMRM dye as compared to the cells that were administered with 75 μM H_2O_2. Considering that TMRM is a dye that collects in the membranes of healthy mitochondria as opposed to the membranes of depolarized mitochondria (Floryk and Houstěk, 1999; Morganti et al. 2019).

In our investigation, hematoxylin and eosin staining was performed to characterize organoid models, and the results revealed distinct cell distribution profiles within the models. On 14th day organoids, cells in the control group organoid models showed a more aggregated profile, resembling neurosphere-like cell clusters, whereas cells in the experimental group organoid models were concentrated at the edge of the model. At 28th day, the differences in cellular distribution between the groups became more pronounced. Neurosphere-like cell clusters observed in the control group's organoid models suggested the maintenance of stem cell characteristics of NSCs in the model, while the distribution of cells in the experimental group was interpreted as an oxidative stress-induced stimulation leading to cell differentiation. Several studies have shown an increase in cell migration capacity when low concentrations of H_2O_2 are applied for preconditioning neural progenitor cells in 2D culture conditions (Sharma et al. 2008).

Our study revealed that the immunofluorescent staining on the 28th day was more intense than that on the 14th day. In particular, the staining for GFAP and NG2, which are glial cell markers, was more intense in the experimental groups compared to the control. In terms of neuronal cell markers, Tubulin Beta III staining was most intense in the experimental group on the 28th day. Given that WNT3A gene expression was also high, this result was expected. To determine the potential of our organoid model for neurodegenerative disease research, we examined the markers for Parkinson's and Alzheimer's diseases. Our findings showed that TH, the Parkinson's disease marker, was not expressed in the organoid models. However, Tau, one of the Alzheimer's disease markers, was positive in the organoid models as a result of immunofluorescent staining, and the staining was weaker in the experimental group only on the 28th day compared to the control group. The difference in staining profiles in this group can be attributed to the high WNT3A expression, as it is known that increased WNT3A gene expression reduces neurodegeneration caused by beta amyloid fibrils, which are seen in Alzheimer's pathology, and thus affects the course of the disease (De Ferrari et al. 2003; Arrázola et al. 2015).

The activity of SOD enzyme was assessed in organoid models as a marker of oxidative stress. Since the concentration of antioxidants in the environment increases in response to the balancing of oxidative agents caused by stress in the cell, it was concluded that H_2O_2 had the desired effect on the cell. In the 1st day organoid models, the SOD enzyme activity was only observed in the experimental group, indicating that H_2O_2 had the desired effect

in the cell. It was determined that the increased SOD enzyme activity in the 14th day control organoid model compared to the 1st day was due to the formation of an oxygen-free zone due to the central localization of the cells in the model. The increase in SOD activity in the 14th day experimental group suggests that the effects of oxidative stress-induced cellular stimulation are ongoing, and the cellular distribution profile revealed by hematoxylin and eosin staining supports this result. In the 28th day organoid models, there was a decrease in SOD activity in both groups, indicating that the oxidative stress created by H_2O_2 loses its effectiveness on cells. The assessment of mitochondrial membrane potential was carried out using TMRM staining in organoid models. The control group showed more prominent staining on the 1st day due to the cationic nature of TMRM dye, which accumulates in healthy mitochondria. By 14th day, both groups revealed similar staining patterns, suggesting an increase in cell number and healthy cells, along with an increase in SOD enzyme activity and total protein content in both groups. However, on the 28th day, the experimental group demonstrated more intense TMRM staining than the control group. This difference may be attributed to the deterioration of cells in the control group resulting from oxidative stress, as SOD enzyme activity was higher in the control group on the 28th day.

After performing the TMRM staining process, we conducted Mitotracker Red staining to determine the total amount of mitochondria in the organoid models. The results revealed that in the 1st day organoid models, the experimental group showed weaker staining compared to the control group, potentially due to the oxidative stress induced on the cells, which led to mitophagy and a decrease in the number of mitochondria in the cells (Dolman et al. 2013; Barbour and Turner, 2014). This reduction in mitochondrial biogenesis and mitophagy is associated with various diseases, including Alzheimer's, Type 1 Diabetes Mellitus, and aging (Wallace, 1999; Jornayvaz and Shulman, 2010). In contrast, the staining in the 14th day organoid models was comparable between both groups, possibly due to the absence of stressors affecting the cells forming the organoid models. However, in the 28th day organoid models, the experimental group exhibited more intense staining with Mitotracker Red dye than the control group. This intensity may be attributed to mitophagy caused by oxidative stress resulting from a change in the mitochondrial membrane potential due to oxygen deprivation caused by cellular distribution in the 28th day control organoid model.

The examination of gene expression levels in organoid models revealed that the SHH gene, which is a component of the Hedgehog signaling pathway and is known to provide stimulation of antioxidative effects such as preventing ROS formation under oxidative stress conditions, preventing mitochondrial damage, and increasing ATP production, was found to be high in the 28th day experimental group (He et al. 2017; Chen et al. 2018). This expression of SHH supports the intense mitotracker staining observed in the same group. These results indicate that a cellular response against oxidative stress occurred in the organoid structure of the experimental group on the 28th day. The expression profile of the WNT3A gene, which is involved in cellular differentiation processes, indicates neural differentiation (Muroyama et al., 2004). The high expression level of the experimental group on the 28th day indicates that the oxidative stress created for this experimental group directs neuronal differentiation. At the same time, the increase in WNT3A gene expression level reduces the neurodegeneration caused by beta amyloid fibrils seen in Alzheimer's pathology and thus affects the course of the disease (De Ferrari et al. 2003; Arrázola et al. 2015). The high expression level of WNT3A gene in the 28th day experimental group explains the reason for the weak staining of the Tau Alzheimer marker compared to the control. The Notch1 gene belongs to the Type1 transmembrane protein family and has been found to play a role in cellular differentiation processes, particularly in the increased expression of this gene during glial cell differentiation. The results suggest that the

control group exhibits higher levels of glial cell differentiation on 28th day, as the expression level of the control group is higher than the experimental group. The administration of H_2O_2 appears to stimulate specific cell differentiation, as the results imply that it triggers the expression of the Notch1 gene. The observation of similar expression of the Noggin gene in both groups, which directs neural and glial cell differentiation through the expression of BMP profiles, indicates that the spontaneous cell differentiation that occurs is successful. These findings support the conclusion that H_2O_2 administration stimulates specific cell differentiation. (Hojo et al. 2000; Grandbarbe et al. 2003; Morell et al. 2015).

The outcomes of the oxidative stress markers SOD1 and HO1 genes for the experimental groups were found to be higher than those of the control groups, indicating that the intended increase in oxidative stress through the use of H_2O_2 was successful. The opposing expression profile of RAGE in comparison to SOD1 and HO1 supports these results. The biochemical analysis kit used to analyze SOD further corroborates the gene expression findings. Peak expression was observed in the experimental group on 14th day, after which it began to decrease. The high expression of DUOX1 in the experimental group on 28th day suggests a significant accumulation of ROS in the model. A number of studies have also shown that DUOX1 stimulates cell migration in various cell types, especially immune cells, in response to environmental changes (Balta et al. 2020; Kennedy et al. 2010). When the researchers examined the influence of oxidative stress on the expression of the MCT-4 gene, they discovered a direct correlation. The upregulation of the MCT-4 gene typically indicates mitochondrial damage. The NRF2 gene is crucial for the maintenance of mitochondrial biogenesis and mitochondrial reactive oxygen species (ROS) homeostasis, and reduced NRF2 gene expression has been associated with a decrease in the number of mitochondria, disruption of mitochondrial biogenesis, and mitophagy processes (Chen et al. 2012; Barbour and Turner, 2014). The higher expression profile observed on the 28th day in the experimental group in comparison to the control group confirms the mitotracker red staining. NOD2, which has a role in autophagy and apoptosis, contributes to cellular survival by inducing the expression of antiapoptotic proteins. Furthermore, NOD2, much like NRF2, has been found to be involved in mitophagy processes (Lupfer et al. 2013; Maurya et al. 2015; Levy et al. 2020). The subunits NOX4 and P22phox, both part of the NOX family, function as oxygen sensors and catalyze the reduction of oxygen into various reactive oxygen species (ROS). These ROS are involved in cellular signal transduction and differentiation. Research has indicated that an increase in NOX4 expression is correlated with increased oxidative stress and mitochondrial dysfunction, while a decrease in the gene's expression suggests a reduction in stress. (Vendrov et al. 2015). The finding of low NOX4 expression in the experimental groups on the 14th day was interpreted as being due to the high antioxidant levels in these groups. This is because an increase in antioxidant levels creates a balance with the oxidants, leading to a decrease in cellular stress and a decrease in NOX4 expression.

The results of the BCA analysis for evaluating the total protein content in organoid models showed that the protein levels in the experimental groups were greater than those in the control groups. Moreover, the peak value achieved on 14th day decreased due to the degradation and destruction of the matrigel, which served as the support structure. This decrease in protein amount is also suggestive of the reorganization of the microenvironment that we anticipate observing in organoids. As this regulation involves the ongoing secretion of proteases and tissue-specific structural proteins, it is expected to fluctuate over time. In conclusion, H_2O_2 plays a crucial role in guiding specific cell differentiation processes and influencing cell behavior. These findings were validated through gene expression analysis, histological examination, and immunofluorescent and biochemical assessments. The effects

of hydrogen peroxide on cells varied depending on the concentration levels, and at the specified dose, it promoted cell growth by facilitating cell differentiation. The organoid model developed in this study demonstrates potential for use in Alzheimer's disease treatment. The model showcases the migration and differentiation of natural killer cells, and initial characterization of the differentiated cells has been conducted. Further research is required to provide a comprehensive description of the organoid model and its constituent cells.

Acknowledgements This work was supported by the Scientific Research Projects Coordination Unit of Kocaeli University for their financial backing of this study through the KOU-BAP project, which has the project number TYL-2020-2215 and we would like to express our thanks to them for this so-called support. In addition, we would like to express my gratitude to Prof. Dr. Ayşe Karson for her invaluable aid in utilizing the criomicrotome device during sectioning.

Author Contributions

Conceptualization: [Onur Özcan and Yusufhan Yazır]; Methodology: [Onur Özcan, Yusufhan Yazır, and Gökhan Duruksu]; Formal analysis and investigation: [Onur Özcan, Ahmet Öztürk, Kamil Can Kılıç and Gökhan Duruksu]; Writing - original draft preparation: [Onur Özcan and Kamil Can Kılıç]; Writing - review and editing: [Onur Özcan and Kamil Can Kılıç]; Funding acquisition: [Yusufhan Yazır]; Resources: [Onur Özcan and Yusufhan Yazır]; Supervision: [Yusufhan Yazır].

Statements and Declarations

Conflict of interest The authors have declared no financial or non-financial conflicts of interest.

References

Abdanipour A, Jafari Anarkooli I, Shokri S, Ghorbanlou M, Bayati V, Nejatbakhsh R (2018) Neuroprotective effects of selegiline on rat neural stem cells treated with hydrogen peroxide. Biomed Rep 8(1):41–46. https://doi.org/10.3892/br.2017.1023

Arrázola MS, Silva-Alvarez C, Inestrosa NC (2015) How the Wnt signaling pathway protects from neurodegeneration: the mitochondrial scenario. Front Cell Neurosci 9:166. https://doi.org/10.3389/fncel.2015.00166

Balta E, Kramer J, Samstag Y (2021) Redox Regulation of the Actin Cytoskeleton in Cell Migration and Adhesion: On the Way to a Spatiotemporal View. Front Cell Dev Biol 8:618261. https://doi.org/10.3389/fcell.2020.618261

Barbour JA, Turner N (2014) Mitochondrial stress signaling promotes cellular adaptations. Int J Cell Biol 2014:156020. https://doi.org/10.1155/2014/156020

Berlett BS, Stadtman ER (1997) Protein oxidation in aging, disease, and oxidative stress. J Biol Chem 272(33):20313–20316. https://doi.org/10.1074/jbc.272.33.20313

Cadet J, Douki T, Pouget JP, Ravanat JL, Sauvaigo S (2001) Effects of UV and visible radiations on cellular DNA. Curr Probl Dermatol 29:62–73. https://doi.org/10.1159/000060654

Chen J, Zhou L, Pan SY (2014) A brief review of recent advances in stem cell biology. Neural Regen Res 9(7):684–687. https://doi.org/10.4103/1673-5374.131565

Chen SD, Yang JL, Hwang WC, Yang DI (2018) Emerging roles of sonic hedgehog in adult neurological diseases: neurogenesis and beyond. Int J Mol Sci 19(8):2423. https://doi.org/10.3390/ijms19082423

Chen X, Guo C, Kong J (2012) Oxidative stress in neurodegenerative diseases. Neural Regen Res 7(5):376–385. https://doi.org/10.3969/j.issn.1673-5374.2012.05.009

Conklin KA (2000) Dietary antioxidants during cancer chemotherapy: impact on chemotherapeutic effectiveness and development of side effects. Nutr Cancer 37(1):1–18. https://doi.org/10.1207/S15327914NC3701_1

De Ferrari GV, Chacón MA, Barría MI, Garrido JL, Godoy JA, Olivares G, Reyes AE, Alvarez A, Bronfman M, Inestrosa NC (2003) Activation of Wnt signaling rescues neurodegeneration and behavioral impairments induced by beta-amyloid fibrils. Mol Psychiatry 8(2):195–208. https://doi.org/10.1038/sj.mp.4001208

Dolman NJ, Chambers KM, Mandavilli B, Batchelor RH, Janes MS (2013) Tools and techniques to measure mitophagy using fluorescence microscopy. Autophagy 9(11):1653–1662. https://doi.org/10.4161/auto.24001

Ekert JE, Johnson K, Strake B, Pardinas J, Jarantow S, Perkinson R, Colter DC (2014) Three-dimensional lung tumor microenvironment modulates therapeutic compound responsiveness in vitro--implication for drug development. PloS One 9(3):e92248. https://doi.org/10.1371/journal.pone.0092248

Ergen SK, Subasi S, Rencber SF, Duruksu G, Yazir Y (2022) Evaluation of clinical and histological effects of KGF-2 and NGF on corneal wound healing in an experimental alkali burn rabbit model. Exp Eye Res 223:109190. https://doi.org/10.1016/j.exer.2022.109190

Finnberg NK, Gokare P, Lev A, Grivennikov SI, MacFarlane AW 4th, Campbell KS, Winters RM, Kaputa K, Farma JM, Abbas AE, Grasso L, Nicolaides NC, El-Deiry WS (2017) Application of 3D tumoroid systems to define immune and cytotoxic therapeutic responses based on tumoroid and tissue slice culture molecular signatures. Oncotarget 8(40):66747–66757. https://doi.org/10.18632/oncotarget.19965

Floryk D, Houstěk J (1999) Tetramethyl rhodamine methyl ester (TMRM) is suitable for cytofluorometric measurements of mitochondrial membrane potential in cells treated with digitonin. Biosci Rep 19(1):27–34. https://doi.org/10.1023/a:1020193906974

Furat Rencber S, Kurnaz Ozbek S, Eraldemır C, Sezer Z, Kum T, Ceylan S, Guzel E (2018) Effect of resveratrol and metformin on ovarian reserve and ultrastructure in PCOS: an experimental study. J Ovarian Res 11(1):55. https://doi.org/10.1186/s13048-018-0427-7

Gage FH (2000) Mammalian neural stem cells. Science 287(5457):1433–1438. https://doi.org/10.1126/science.287.5457.1433

Gitler AD, Dhillon P, Shorter J (2017) Neurodegenerative disease: models, mechanisms, and a new hope. Dis Model Mech 10(5):499–502. https://doi.org/10.1242/dmm.030205

Grandbarbe L, Bouissac J, Rand M, Hrabé de Angelis M, Artavanis-Tsakonas S, Mohier E (2003) Delta-Notch signaling controls the generation of neurons/glia from neural stem cells in a stepwise process. Development 130(7):1391–1402. https://doi.org/10.1242/dev.00374

Hammerschmidt S, Wahn H (2004) The oxidants hypochlorite and hydrogen peroxide induce distinct patterns of acute lung injury. Biochim Biophys Acta 1690(3):258–264. https://doi.org/10.1016/j.bbadis.2004.07.003

He W, Cui L, Zhang C, Zhang X, He J, Xie Y, Chen Y (2017) Sonic hedgehog promotes neurite outgrowth of cortical neurons under oxidative stress: Involving of mitochondria and energy metabolism. Exp Cell Res 350(1):83–90. https://doi.org/10.1016/j.yexcr.2016.11.008

Hojo M, Ohtsuka T, Hashimoto N, Gradwohl G, Guillemot F, Kageyama R (2000) Glial cell fate specification modulated by the bHLH gene Hes5 in mouse retina. Development 127(12):2515–2522. https://doi.org/10.1242/dev.127.12.2515

Jaul E, Barron J (2017) Age-Related Diseases and Clinical and Public Health Implications for the 85 Years Old and Over Population. Front Public Health 5:335. https://doi.org/10.3389/fpubh.2017.00335

Jornayvaz FR, Shulman GI (2010) Regulation of mitochondrial biogenesis. Essays Biochem 47:69–84. https://doi.org/10.1042/bse0470069

Kennedy KA, Ostrakhovitch EA, Sandiford SD, Dayarathna T, Xie X, Waese EY, Chang WY, Feng Q, Skerjanc IS, Stanford WL, Li SS (2010) Mammalian numb-interacting protein 1/dual oxidase maturation factor 1 directs neuronal fate in stem cells. J Biol Chem 285(23):17974–17985. https://doi.org/10.1074/jbc.M109.084616

Konyalioglu S, Armagan G, Yalcin A, Atalayin C, Dagci T (2013) Effects of resveratrol on hydrogen peroxide-induced oxidative stress in embryonic neural stem cells. Neural Regen Res 8(6):485–495. https://doi.org/10.3969/j.issn.1673-5374.2013.06.001

Lee BR, Um HD (1999) Hydrogen peroxide suppresses U937 cell death by two different mechanisms depending on its concentration. Exp Cell Res 248(2):430–438. https://doi.org/10.1006/excr.1999.4409

Levy A, Stedman A, Deutsch E, Donnadieu F, Virgin HW, Sansonetti PJ, Nigro G (2020) Innate immune receptor NOD2 mediates LGR5^{+}intestinal stem cell protection against ROS cytotoxicity via mitophagy stimulation. Proc Natl Acad Sci U S A 117(4):1994–2003. https://doi.org/10.1073/pnas.1902788117

Lupfer C, Thomas PG, Anand PK, Vogel P, Milasta S, Martinez J, Huang G, Green M, Kundu M, Chi H, Xavier RJ, Green DR, Lamkanfi M, Dinarello CA, Doherty PC, Kanneganti TD (2013) Receptor interacting protein kinase 2-mediated mitophagy regulates inflammasome activation during virus infection. Nat Immunol 14(5):480–488. https://doi.org/10.1038/ni.2563

Maurya CK, Arha D, Rai AK, Kumar SK, Pandey J, Avisetti DR, Kalivendi SV, Klip A, Tamrakar AK (2015) NOD2 activation induces oxidative stress contributing to mitochondrial dysfunction and insulin resistance in skeletal muscle cells. Free Radic Biol Med 89:158–169. https://doi.org/10.1016/j.freeradbiomed.2015.07.154

McKay R (1997) Stem cells in the central nervous system. Science 276(5309):66–71. https://doi.org/10.1126/science.276.5309.66

Morell M, Tsan YC, O'Shea KS (2015) Inducible expression of noggin selectively expands neural progenitors in the adult SVZ. Stem Cell Res 14(1):79–94. https://doi.org/10.1016/j.scr.2014.11.001

Morganti C, Bonora M, Ito K, Ito K (2019) Electron transport chain complex II sustains high mitochondrial membrane potential in hematopoietic stem and progenitor cells. Stem Cell Res 40:101573. https://doi.org/10.1016/j.scr.2019.101573

Muroyama Y, Kondoh H, Takada S (2004) Wnt proteins promote neuronal differentiation in neural stem cell culture. Biochem Biophys Res Commun 313(4):915–921. https://doi.org/10.1016/j.bbrc.2003.12.023

Oz Oyar E, Aciksari A, Azak Pazarlar B, Egilmez CB, Duruksu G, Rencber SF, Yardimoglu Yilmaz M, Ozturk A, Yazir Y (2022) The therapeutical effects of damage-specific stress induced exosomes on the cisplatin nephrotoxicity IN VIVO. Mol Cell Probes 66:101861. https://doi.org/10.1016/j.mcp.2022.101861

Rende B, Orha AT (2024) Hip Joint Angular Values in Children with Bilateral Spastic Cerebral Palsy: A Comparison between Ambulatory and Nonambulatory Groups According to the Gross Motor Functional Classification System. J Anat Soc India 73(2):145-151. https://doi.org/10.4103/jasi.jasi_137_23

Sangkum P (2016) Research highlights on stem cell therapy for the treatment of Peyronie's disease. Transl Androl Urol 5(3):363–365. https://doi.org/10.21037/tau.2016.03.14

Sharma RK, Zhou Q, Netland PA (2008) Effect of oxidative preconditioning on neural progenitor cells. Brain Res, 1243, 19–26. https://doi.org/10.1016/j.brainres.2008.08.025

Simonian NA, Coyle JT (1996) Oxidative stress in neurodegenerative diseases. Annu Rev Pharmacol Toxicol 36:83–106. https://doi.org/10.1146/annurev.pa.36.040196.000503

Spector A, Ma W, Sun F, Li D, Kleiman NJ (2002) The effect of H2O2 and tertiary butyl hydroperoxide upon a murine immortal lens epithelial cell line, alphaTN4-1. Exp Eye Res 75(5):573–582. https://doi.org/10.1006/exer.2002.2045

Su CY, Chong KY, Edelstein K, Lille S, Khardori R, Lai CC (1999) Constitutive hsp70 attenuates hydrogen peroxide-induced membrane lipid peroxidation. Biochem Biophys Res Commun 265(2):279–284. https://doi.org/10.1006/bbrc.1999.1649

Tang D, Shi Y, Kang R, Li T, Xiao W, Wang H, Xiao X (2007) Hydrogen peroxide stimulates macrophages and monocytes to actively release HMGB1. J Leukoc Biol 81(3):741–747. https://doi.org/10.1189/jlb.0806540

Tekin A, Rende B, Efendi H, Bunul SD, Çakır Ö, Çolak T, Balcı S (2024) Volumetric and Asymmetric Index Analysis of Subcortical Structures in Multiple Sclerosis Patients: A Retrospective Study Using volBrain Software. Cureus 16(3):e55799. https://doi.org/10.7759/cureus.55799

Tokuc EO, Yuksel N, Rencber SF, Ozturk A, Duruksu G, Yazir Y, Ergun RE (2021) Protective effects of citicoline-containing eye drops against UVB-Induced corneal oxidative damage in a rat model. Exp Eye Res 208:108612. https://doi.org/10.1016/j.exer.2021.108612

Valen G, Starkopf J, Takeshima S, Kullisaar T, Vihalemm T, Kengsepp AT, Löwbeer C, Vaage J, Zilmer M (1998) Preconditioning with hydrogen peroxide (H2O2) or ischemia in H2O2-induced cardiac dysfunction. Free Radic Res 29(3):235–245. https://doi.org/10.1080/10715769800300271

Vendrov AE, Vendrov KC, Smith A, Yuan J, Sumida A, Robidoux J, Runge MS, Madamanchi NR (2015) NOX4 NADPH Oxidase-Dependent Mitochondrial Oxidative Stress in Aging-Associated Cardiovascular Disease. Antioxid Redox Signal 23(18):1389–1409. https://doi.org/10.1089/ars.2014.6221

Wallace DC (1999) Mitochondrial diseases in man and mouse. Science 283(5407):1482–1488. https://doi.org/10.1126/science.283.5407.1482

Zakrzewski W, Dobrzyński M, Szymonowicz M, Rybak Z (2019) Stem cells: past, present, and future. Stem Cell Res Ther 10(1):68. https://doi.org/10.1186/s13287-019-1165-5

Zhao C, Deng W, Gage FH (2008) Mechanisms and functional implications of adult neurogenesis. Cell 132(4):645–660. https://doi.org/10.1016/j.cell.2008.01.033